Proceedings World Geothermal Congress 2015
Melbourne, Australia, 19-25 April 2015

Research of Silica Extracted from the Hydrothermal Solutions

Potapov V.V., Shalaev K.S., Gorev D.S., Kashutin A.N., Shunina E.V., Zubaha S.V.

Geotechnological Research Center, Far East Branch of Russian Academy of Science Petropavlovsk-Kamchatsky, Russia, 683002, Severo-Vostochnoe shosse, 30, e-mail: vadim_p@inbox.ru

Keywords: hydrothermal solution, silica sol, membrane concentration, silica nanopowders, concrete

ABSTRACT

Silica sols and powders extracted from hydrothermal solutions have been investigated. Hydrothermal solutions contain the colloidal silica forming as a result of polycondensation of the molecules of orthosilicic acid. Via ultrafiltration membrane concentration of hydrothermal solutions, silica sols with SiO_2 contents up to 940 g/dm^3 (62.2 wt %) and particle radii of 29-135 nm are obtained. The silica powders with the specific surface of 50-500 m^2/g, average pore diameter of 3-12 nm, and pore volume of 0.2-0.3 cm^3/g are obtained via cryochemical vacuum-sublimation drying of sols with the use of liquid nitrogen. Silica sols and powders were used as additivities for rising concrete compressive strength.

1. INTRODUCTION

The development of technologies for preparing nanomaterials with various properties dictates the necessity to investigate the influence of introduced nanoparticles on the properties of silicate systems (Eletskii, A.V, 2000). A change in the characteristics of materials is achieved as a result of either the change in the amount and chemical composition of introduced nanoparticles or the simultaneous introduction of a combination of nanoparticles with different chemical compositions. The problems associated with the controlled improvement of properties of structural concretes, such as the compressive and bending strengths, waterproofing, frost resistance, etc., as well as with the influence on the characteristics of other building materials, including binders (cement, gypsum, lime), glasses, sealants, and heat insulators, are of considerable interest.

There are experimental data on the use of fulleroids in the production of foam and gas concrete blocks, according to which the strength of conventional blocks increases bv 16–18% and their densitv decreases bv 8–10% when the concentration of fullerene-like compounds is equal to 1 – 10 g per concrete ton. Moreover, this also leads to a shortening of the production cycle(Ponomarev, A.N., 2001).

Strotskii et al. (Strotskii V.N. et al., 2008) showed that, in the production of concrete, the introduction of 10 to 50 nm carbon nanoparticles in amounts of 0.004 wt *%* with respect to the cement improved the influence of the silica microadditive (8 wt 96) and increased the compressive strength of the concrete to 104.5 MPa, which corresponds to the V80 concrete rather than to the V60 concrete. This also led to a significant increase in the elastic modulus (47.5 x 10^3 MPa). Poisson's ratio, density, and waterproofing of the concrete. There disappeared an increase in the concrete shrinkage, which with the use of one microsilica additive reached 30%.

In (Shitikov E.S. Strotskii. V.N. and Gordeeva E.V., 2008) the authors investigated the influence of nanomaterials on the strength of concretes prepared from cements of different types: (1) carbon nanoparticles with sizes of 5–20 run in the form of a 5% aqueous sol; (2) powders of nanoparticles of a mixture of Al_20_3, CaO, and MgO oxides with sizes of 10–50 nm; and (3) W and Ti nanoparticles with sizes of 10–50 nm. The authors studied the possibility of using both carbon nanoparticles and different plasticizers of the concrete. In (Shitikov E.S. Strotskii. V.N. and Gordeeva E.V., 2008), it was established that the concrete strength varies (increases or decreases) nonmonotoni-cally depending on the amount of introduced nanoparticles. The first maximum of the strength was observed in the range of low concentrations (0.0007– 0.0014 wt *%)* with respect to the cement.

There are examples of the preparation of high-strength concretes with a higher fraction of combined nanoadditives: the introduction of silica sol (0.43–0.48 wt *%* with respect to concrete) with a density of 1014 g/dm^3, pH 5–6, and $Si0_2$ content of 26–27 g/dm^3 together with an organomineral nanoadditive (0.43–0.48 wt *%)* leads to an increase in the strength of concrete bv *42%* and in the water-proofing by two grades (Svatovskaya, L.B. et al., 2004). The introduction of silica sol (0.25–0.27 wt *96* with respect to concrete) with a density of 1014 g/dm^3, pH 5–6, and $Si0_2$ content of 26–27 g/dm^3 together with a nanoadditive in the form of potassium hexacyanoferrate $K_4Fe(CN)_6$ (0.44–0.47 wt *%)* results in a simultaneous increase in the strength of concrete by 31 %, frost resistance by 35%, and waterproofing by 20% (Svatovskaya, L.B. et al., 2004). The introduction of an iron hydroxide ($Fe(OH)_3$) sol with a density of 1021 g/dm^3 and pH 4.5 together with potassium hexacyanoferrate $K_4Fe(CN)_6$ and superplasti-cizer (total content of 0.6–0.8 wt % with respect to concrete) increases the strength of concrete by 61% and decreases the water demand by 23% and the creep by 30% (Korobov N.V., Kotorazhuk Ya.D.and Starchukov, D.S., 2007).

Roddy et al. (Roddy, C.W. et al., 2009) proposed to add silica nanoparti-cles (to cements) with sizes from 1 to 100 nm in amounts from 1 to 25 wt % with respect to cement in order to improve the characteristics of solutions for plugging of the well, drilling fluid, etc. In (Roddy, C.W. et al., 2009), the authors reported on the results of experiments on a comparative study of solidified samples of water-cements mixtures into which different type of silica were introduced in amounts of 15 wt % with respect to cement: silica nanoparticles 10 and 30 nm in size, amorphous and crystalline microsilicas, and colloidal silica (Roddy, C.W. et al., 2009). The best results were obtained when introducing silica nanoparticles 30 nm in size. The setting time of the water–cement mixture was reduced bv a factor of 5–7 as compared to microsilica. The compressive strength at the age of three days was higher by a factor of 1.5–2.0 (2.95 MPa), and the bending strength was higher by a factor of 1.7–4.0 (1.16 MPa). After the final strength development, the samples formed from mixtures with introduced silica nanopar-ticles 30 nm in size had a compressive strength that was 2.4–3.0 times higher as compared to microsilica (8.27 M Pa), the Young's modulus was 1.5 times higher than that for crystalline microsilica (2.15 x 10^5), and the Poisson's ratio was 1.5 times higher than that for samples containing amorphous or crystalline micro-silica (0.1).

In this respect, it is of interest to investigate the influence of nanoparticles (different in their chemical composition and properties, such as the size, shape, internal structure, and surface conditions) on systems of the cement–water, cement–sand–water, and cement–sand–water–concrete types: the position of maxima and minima in the dependences of the strength, density, elastic modulus, and Poisson's ratio; the time characteristics of the strength development; etc. The aim of this work is to investigate the influence of silica nanoparticles separated from hydrothermal solutions according to the two-stage scheme on a system of the cement–sand–water type.

2. EXTRACTION OF SILICA AND RESEARCH SILICA CHARACTERISTICS

In order to prepare silica nanoparticles, natural hvdrothermal solutions were used as the initial medium. Under conditions of elevated pressures and temperatures, orthosilicic acid molecules are formed in depths of deposits due to the dissolution of alumi-nosilicate minerals of rocks in hvdrothermal solutions. After the escape to the surface, the pressure and temperature decrease, the solution become supersaturated, and there occur hydrolysis and polycondensa-tion of orthosilicic acid molecules in this solution, which lead to the formation of spherical silica nanoparticles 5–100 nm in radii. Apart from silica, the initial solution contains other components with the concentrations listed in Table 1.

Table 1. The concentration of the main components of the initial hydrothermal solution

Component	Na^+	K^+	Li^+	Ca^{2+}	Mg^{2+}	$Fe^{2+,\,3+}$	Al^{3+}
Concentration, mg/l	282	48.1	1.5	2.8	4.7	<0.1	<0.1
Component	Cl^-	SO_4^{2}	HCO_3^-	CO_3^{2-}	H_3BO_3	SiO_2	Cl^-
Concentration, mg/l	251.8	220.9	45.2	61.8	91.8	780	251.8

The polycondensation of silicic acid molecules proceeds as a result of the condensation of silanol groups, the formation of siloxane bonds, and partial dehydration. The final sizes of silica particles, depend primarily on the temperature and pH at which there occurs polycondensation of orthosilicic acid molecules. An increase in the polycondensation temperature leads to an increase in the final sizes of particles. A decrease in the pH, like the increase in the temper temperature, results in the increase in the final sizes of particles. At the polycondensation stage, the temperature was varied from 20 to 72°C and the pH was varied from 9.2 to 4.0. In this case, the final average radii of silica particles varied from 5 to 60 nm depending on the temperature and pH.

After the completion of the polycondensation of orthosilicic acid in hvdrothermal solutions and the formation of silica nanoparticles with specific sizes, water was removed in order to prepare nanodispersed powders. Water was removed using the two-stage scheme (Potapov, V.V. et al., 2008, Generalov M.B., 2006, Brazhnikov S.M., Generalov M.B., and Taitnev N.S., 2004):

(1) at the first stage, filtering through membrane devices; and
(2) at the second stage, cryochemical vacuum sublimation drying with the use of liquid nitrogen.

The specific energy consumption for the preparation of the silica powder per unit mass was E_m = 21.2– 7.3kWh/kg.

A setup for the membrane concentration of the hydrothermal solution involved a cartridge (cartridges) with membrane filters; pump; flow meters; shut-off and control valves; and tanks for the initial solution, concentrate, and filtrate. In experiments, we studied the possibility of using the main technological processes of membrane separation for the concentration of hydrothermal solutions: microfiltration, ultrafiltration, and reverse osmosis. The main technological processes of membrane separation differ, primarily, in the use of filters with different pore diameters in the membrane layer: reverse osmosis, 0.1– 1.0 nm; ultrafiltration, 1.0–50.0 nm; and micro-filtration, 50-10000 nm.

In the use of ultrafiltration, the silica nanoparticles were retained by the membrane layer, whereas water molecules and ions of dissolved salts passed through it. Therefore, the electrolyte content decreased during the concentration of silica, which provided the stability of sols. The experiments with membranes demonstrated the advantage of ultrafiltration for the preparation of stable concentrated silica sols. In the use of the reverse osmosis, the concentration of silica was accompanied by an increase in the ion content and the prepared sols were unstable. Microfiltration membranes have a low selectivity with respect to silica nanoparticles and cannot be effective at the first stages of concentration at low SiO. contents. In this respect, the ultrafiltration or a combination of ultrafiltration and microfiltration was used in the majority of case for the accumulation of considerable amounts of sols: at the first stage, ultrafiltration and, at the next stages, microfiltration. In this case, we used ultrafiltration membranes of the capillary type in which polyether-sulfone and poly(acrylonitrile) served as materials of the membrane laver. The initial medium is fed into long capillary tubes, in which walls represent a membrane layer. In motion inside the tube, a part of the medium filtrates to the outside in the radial direction and accumulates in the housing of the filter cartridge in the space between tube (filtrate). The part of the medium that passed over the entire length of the tube without filtering through the membrane walls (concentrate) is fed to the collector of the concentrate and removed from the cartridge in the axial direction. The filtrate is removed from the housing of the filter cartridge in the lateral direction. The sizes of pores in the membrane layer vary from 20 to 100 nm. We used ceramic microfiltration membranes of the tubular type with an average pore diameter of 70 nm. The concentration was performed in three stages: the SiO-, content was equal to 3–10 g/dm^3 at the first stage, 10– 30 g/dm^3 at the second stage, and 100-840g/dm^3 (10.0-55.0 wt %) at the third stage, and the fraction of water decreased to 90–45 wt %. The density of the sols was equal to 999–1510 g/dm^3, the dynamic viscosity amounted to 1–150 mPa s, the silica particle radii were 5–135 nm. and the zeta potential of particles varied from –32.4 to –42.5 mV. The concentrated aqueous sols with a high $Si0_2$ content were subjected to cryochemical vacuum sublimation drying.

The data on the preparation conditions, average radii, and zeta potentials of silica particles in sols for one of the experimental series are presented in Table 2. The sizes were determined by photon correlation spectroscopy, and the zeta potentials were determined using electrophoresis. The sizes and zeta potentials were measured on a Malvern Zeta-Sizer instrument. In this series, the silica sols were prepared at different values of the temperature (72-30°C) and pH (9.2-4.5) (Table 2). The sol corresponding to the UF17 sample was prepared by the concentration of the separate subjected to aging at a temperature of 72°C. The separate for the UFI8and UF19 sols was subjected to two-stage aging: initially, at 72–70°C, followed by cooling to 50 and 30°C. The cooling of the separate only slightly affected the particle size, because the particles were predominantly formed at an increased temperature of 72–70°C. However, eventually, the particles in the UF19 sol are Iarger than those in the UF17 and UFI8. This is explained by the fact that the U F19 sol was produced using the dead-end scheme of filtration when the inlet for the concentrate was cut off and the concentrated medium was repeatedly recycled through the filter cartridge, which led to the aggregation of silica particles. The sizes of particles in the UF20sol are larger than those in the other sols due to the lower value of the pH at the aging stage of the separate.

Table 2. Results of the determination of the size and the zeta potential of the surface of silica nanoparticles in aqueous sols.

Sample	Conditions for aging of the separate before pressure membrane concentration		Average particle radius in the silica sol before cryochemical drying, nm	Zeta potential of the particle surface, mV
	Temperature, ^{0}C	pH		
UF17	72	9,2	29,5	-39,5
UF 18	70-50	9,2	29,5	-43,8
UF 19	70-30	9,2	55,5	-56,0
UF 20	30	4,5-5,0	135,0	-45,2

The concentrated aqueous silica sols were used to produce weakly aggregated nanodispersed powders. The cryochemical vacuum sublimation drying includes the following sequence of the main technological stages:

- preparation of the concentrated aqueous silica sol;
- dispersion of the sol into droplets and crystallization of droplets in liquid nitrogen at a temperature of 77 K;
- sublimation removal of the solvent from cryo-granules formed at the previous stage so that ice evaporates without melting and passing through the liquid phase; and
- utilization (desublimation) of the solvent, i.e., the condensation of water vapor, and the removal of condensation products from the setup.

The dispersion of aqueous sols into individual droplets is used for producing developed interfaces that ensure a high cooling rate in contact with liquid nitrogen. This cooling rate is necessary in order to prevent the aggregation of silica nanoparticles contained in the initial sol. Moreover, a large surface area of cryo-granules results in an increase in the sublimation rate of ice. Subsequently the sublimation removal of water leads to the formation of weakly aggregated silica powder with the dispersity corresponding to the dispersity of silica in the aqueous sol. The stage of ice sublimation was performed at a pressure lower than the pressure of the triple point of water, which corresponds to the pressure p = 610 Pa and the temperature T = 0.0076°C. As a result, the agglomeration of the silica particles formed at the freezing stage was reduced to a minimum due to the elimination of droplet moisture. At the sublimation stage, the heat expended in evaporating ice was supplied to the through the conductive heat transfer (thermal conductivity).

According to the scanning electron microscopy data at a magnification of 250– 7000, the sizes of sol cryogranules formed as a result of the vacuum sublimation drying lie in the range 20.0–100.0 urn Figures la–Id show the images of the structures of the powder after the sublimation of the solvent at sequentially increasing magnifications of 247, 500, 800, and 1000: the porous network structure that retains features of the spherical shape and sizes of solid cryogranules is formed after the removal of the solvent. The removal of the solvent is accompanied by the formation of cavities in the residual structures in their central part, which indicates the removal of water from solid cryogranules (Fig. 1d). A weak action led to the fracture of the residual structures with the formation of flakes 0.1-0.2 цт thick (Figs, le. 1f).

The size, shape, and structure of particles in the silica powders were determined using scanning electron microscopy. The images of silica nanoparticles in the powders were obtained on a JEOL JEM-100CX scanning electron microscope (Japan) at magnifications of 10000–500000. The powders were preliminarily dispersed in absolute ethanol, the concentrated medium was applied to a copper plate, and the dispersing medium was sublimated. The images of silica powder particles, which were obtained with the scanning electron microscope at sequentially increasing magnifications of 25000, 50000, 100000, and 250000, are displaced in Fig. 2. The cryochemical drying of sols in liquid nitrogen at a temperature of 77 K with the subsequent sublimation of ice undervacuum made it possible to considerably reduce the aggregation of particles when separating silica from the liquid phase. The particles did not coalesce, and the sizes of particles in the sol differed little from the sizes of particles in the powder. It was revealed from the images that, for the most part, the sizes of particles in the sols and powders lie in the range 10–100 tun.

(a)

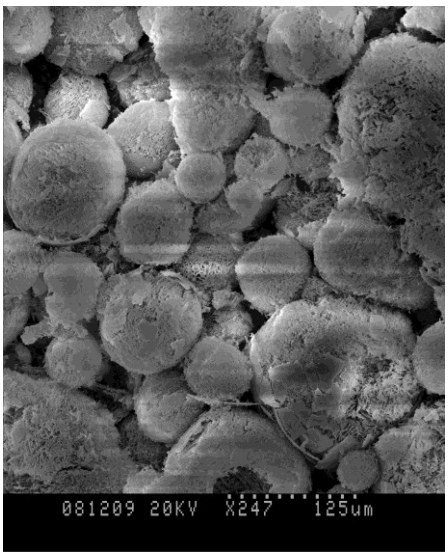

(b)

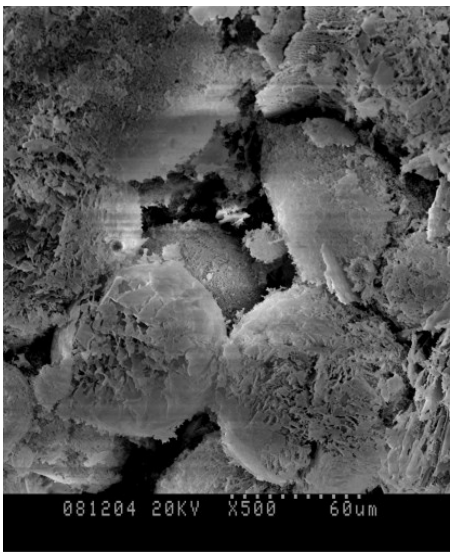

Figure 1 a,b: Cryogranules of the powder obtained by vacuum-sublimation drying of silica sol, magnifications: a) 247; b) 500;

(c)

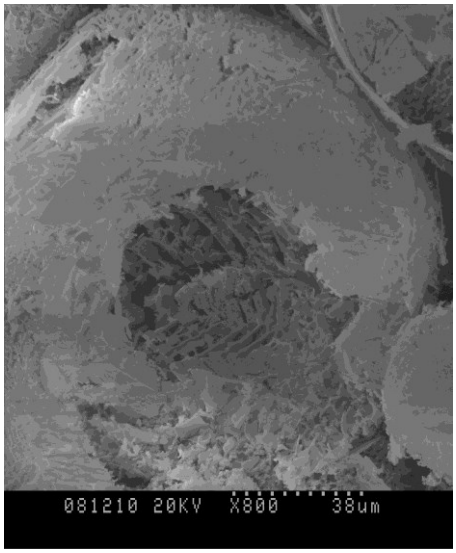

(d)

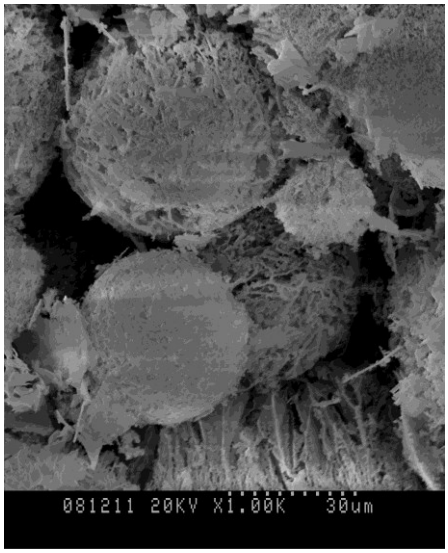

Figure 1 c,d: Cryogranules of the powder obtained by vacuum-sublimation drying of silica sol, magnifications: c) 600; d) 1000;

(e)

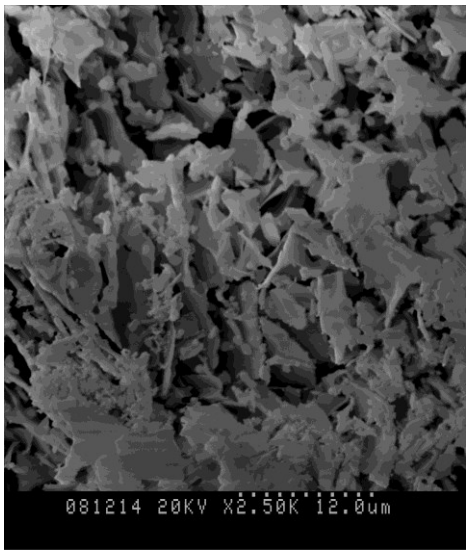

(f)

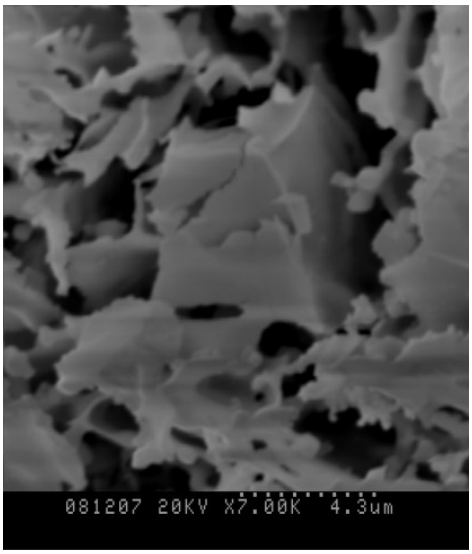

Figure 1e,f : Cryogranules of the powder obtained by vacuum-sublimation drying of silica sol, magnifications: e) 2500; f) 7000;

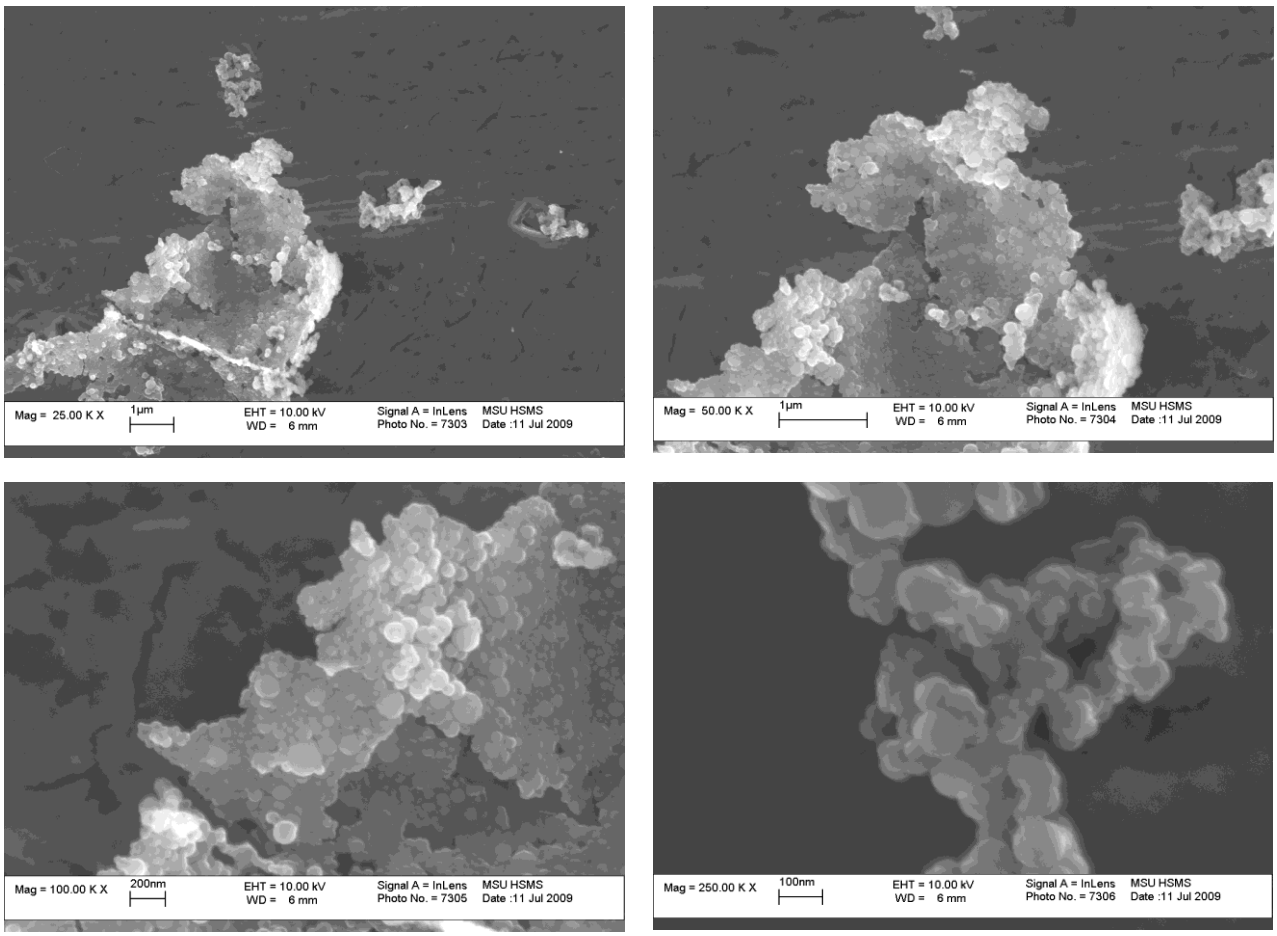

Figure 2: Scanning electron microscope images of the silica powder. Magnification of the scanning electron microscope: (a) x25000, (b> x50000, (c) x 100000, and (d) x250000.

The X-ray powder diffraction data are presented in Figs. 3a and 3b. It can be seen from these figures that the powder has an amorphous structure (Fig. 3a) and, after heat treatment at 1000°C, crystallizes into cristo-balite (Fig. 3b).

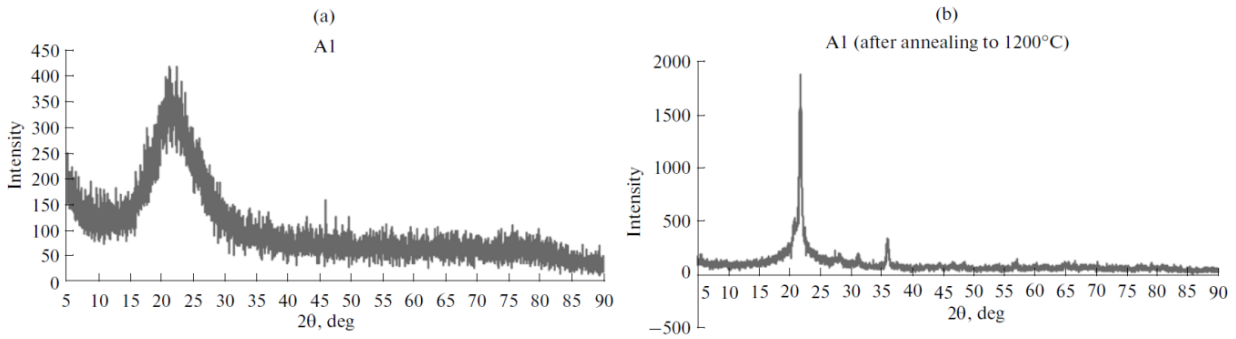

Figure 3: X-ray powder diffraction patterns of the UF20 powder (a) before heat treatment and (b) after heat treatment (ARLX'TRA diffractometer; CuK_α radiation; wavelength, 1.54 Å).

The data on the low-temperature nitrogen adsorption were obtained on a Micromeritics ASAP-2010 porosimeter (Table 3). In different series of experiments, we succeeded in preparing the powders with a high specific surface area from 110–170 to 300– 400 m^2/gand a specific pore volume of 0.2–0.3 enr/g-The bulk density of the powders was equal to 0.035– 0.010g/cm\ The hydrogen index pH at which the aging of the initial hydrothermal solution and subsequent membrane concentration of the sol were performed is one of the main factors that affect the characteristics of the powder. A decrease in the pH value resulted in an increase in the sizes of particles in the sol before the cryochemical doing. Larger porous particles with a developed inner structure were formed so that, after the cryochemical drying of the sol, the specific surface area of the powder became larger. According to the low-temperature nitrogen absorption data, the decrease in the pH value also led to a decrease in the average pore diameter in the powder (Table 3).

Furthermore, the decrease in the pH value resulted in a change in the type of the adsorption–desorption isotherm and the hysteresis loop. The average pore diameters varied from 3.0 to 7.1 nm.

Table 3. Characteristics of pores of silica powders prepared by cryochemical drying of sols

Sample	Density of the powder, g/cm^3	Specific surface area S_{BET}, m^2/g	Average pore diameter d_p nm	Total pore volume V_p, cm^3/g
UF17	0.035	166.5	6	0.259
UF18	0.010	115.0	7	0.204
UF19	0.010	118.3	8	0.230
UF20	0.016	360.4	3	0.301

The smallest value of the average pore diameter in the powders prepared by drying the silica sols with pH 4–5 was approximately equal to 3 nm. The largest value of the average pore diameter (9.6 nm) was observed by drying the sol with pH 9.0–9.2.

The powder introduced as a nanoadditive into cement samples had the specific surface area S_{BET} = 156 m^2/g, the average pore diameter $d_p = l$ nm, and the total pore volume V_p = 0.298 cm^3/g

3. TESTS OF CONCRETE SAMPLES WITH EXRACTED SILICA

The samples under investigation in the form of bars 40 x 40 x 160 mm in size were prepared from a solution that contained cement and sand in a weight ratio of 1 : 3 and had a water–cement ratio of 0.4 *(GOST* (State Standard) 310.4-81). We used the 500DO portland cement. The initial cements represents a finely dispersed powder with a specific surface area of 2250 cm^2/g and a dominant particle size in the range 5–50 (im: the particle size is less than 35 jim for 90% of particles and 5 jim for 10% of particles. The silica powder was introduced into the aqueous phase before the mixing with cement and sand; in this case, a uniform distribution of powder particles over the liquid volume was provided using ultrasonic treatment. A cement–sand mixture was formed by mixing cement and sand. Water was added to the cement–sand mixture, allowing water to be absorbed, and the cement mortar was prepared by their mixing. The cement mortar was placed in molds with a standard shape, which were mounted on a vibrating table for treatment. After the preparation, the samples were removed from molds and stored in baths with water until a particular age was reached. The samples were tested for strength at the ages of 3, 7, and 28 days. The bars were preliminarily tested for the bending strength. and then immediately the halves of the bars were tested for the compressive strength.

The experiments showed that the addition of the nanodispersed silica in amounts of the order of a few thousandths of a weight percent with respect to concrete leads to a significant increase (up to 30–40%) in the compressive strength of the cement samples (see Table 4 in which the corresponding values of the increment of the strength as compared to the check samples without nanoadditive at the same age are given in parentheses).

The characteristic feature of nanodispersed additives is that the dependence of the increase in the strength on the weight percent of the additive exhibits a nonmonotonic behavior. Unlike traditional modifiers, the curve characterizing the strength as function of the weight percent of the nanoadditive has maxima and minima (Table 4). The relative increment of the compressive strength has a tendency toward a decrease with an increase in the sample age. The increment of the compressive strength at the ages of 3 and 7 days is larger than that at the age of 28 days (Table 4. Fig. 4).

The density of the solid cement samples, as a rule, varied in the same manner as the compressive strength: it increased with an increase in the strength. The exception is provided by the sample with 0.04 wt % of the additive. For this additive, the compressive strength increased and the density decreased: p = 1970 kg/m^3 for 0 wt %, 2000 kg/m^3 for 0.0075 wt %, 1920 kg/m^3 for 0.0400 wt %, and 1990 kg/m^3 for 0.1800wt%.

Table 4. Results of the determination of the compressive strength (MPa) of cement samples.

Sample age, days	Amount of added nanodispersed silica, wt,% with respect to cement			
	0	0.0075	0.04	0.18
3	21.5	32.7 (+52.1%)	27.5 (+27.9%)	35.6 (+65.6%)
7	30.8	46.6 (+51.3%)	43.8 (+42.2%)	47.8 (+55.2%)
28	42.7	59.1 (+38.4%)	50.4 (+18.0%)	59.0 (+38.1%)

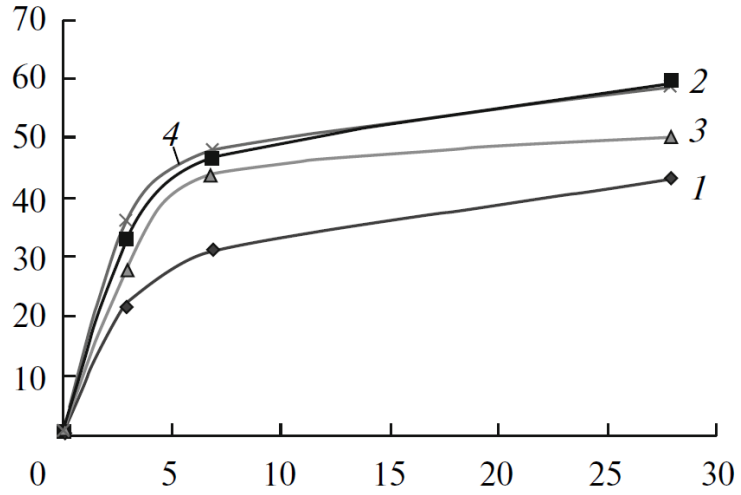

Figure 4: Curves of the increase in the compressive strength of the samples (%) as a function of the age (days): (*1*) without additive, (*2*) 0.0075 wt %, (*3*) 0.04 wt %, and (*4*) 0.18 wt %.

The introduction of silica nanoparticles favored not only the increase in the final compressive strength. This also led to an increase in the rate of strength development for the samples with nanoadditives (Table 5, Fig. 5).

Table 5. Strength development of the cement samples (in percentage terms with respect to the age of 28 days).

Sample age, days	Amount of added nanodispersed silica, wt,% with respect to cement			
	0	0.0075	0.04	0.18
3	50.3	55.3	54.5	60.3
7	72.1	78.8	86.9	81.0
28	100.0	100.0	100.0	100.0

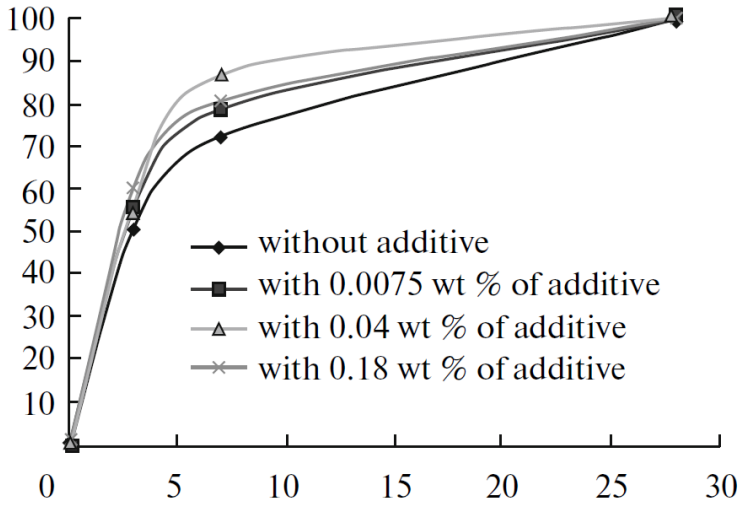

Figure 5: Curves of the development of the compressive strength of the cement samples (in percentage terms with respect to the age of 28 days) as a function of the age (days).

4. CONCLUSIONS

Thus, it has been demonstrated that SiO. nanopar-ticles separated from natural hydrothermal solutions through the developed technological scheme substantially affect the properties of the cement–sand–water system. The introduction of $Si0_2$ nanoparticles in the form of the powder (size of particle aggregates. 10-100 nm; average pore diameter, 3–10 nm; specific surface area, 100–400 m^2/g; zeta potential of the particle surface, from –32.4 to –42.5 mV) into the cement-sand–water system leads to an increase in the compressive strength of solid samples beginning with a few thousandths of a weight percent with respect to concrete. The dependence of the increase in the strength on the nanoadditive content exhibits a nonmonotonic behavior with maxima and minima.

The rate of development of the compressive strength increases upon introduction of the nanoadditive: the strength of the samples containing the nanoadditive increases more rapidly than that of the check samples without nanoadditives.

The density of solid cement samples varies in a nonmonotonic manner as a function of the nanodis-persed silica content and, for the most part, follows the curve of the increase in the compressive strength. For specific nanoadditive contents, the density increases or decreases as compared to the check samples.

The results obtained can be used in construction technologies for structuring cement materials and improving their characteristics, such as the strength, density, waterproofing, and frost resistance.

REFERENCES

Eletskii, A.V., Endohedral Structures. Usp. Fiz- Nauk, 2000. vol. 170, no. 2, pp. 113-142 [Phys.-Usp. (Engl. transi.), 2000, vol. 170, no. 2, pp. 111-1371.

Ponomarev, A.N., Promising Structural Materials and Technologies Designed with the Use of Nanodispersed Fulleroid Systems, Vopr. Materialoved., 2001. no. 2, p. 65.

Strotskii, V.N., Gordeeva, E.V., Vas'kin, V.M., Shitikov, E.S., and Fedorov, E.V., Investigation of Physi-comechanical Properties of High-Strength Concrete with Addition of Microsilica and Ultradispersed Carbon Additive with Nanoparticles 10–50 nm in Size, in Nauchnye trudy OAO TsNIIS(Nauchno-issledovaleVskii institut iransporinogo stroiiel'stva) (Transactions of the OAO Research Institute of Transport Construction), Tsernant. A.A., Ed., Moscow: Research Institute of Transport Construction, 2008, pp. 33–40.

Shitikov, E.S., Strotskii. V.N. and Gordeeva, E.V, On the Possibility of Using Nanomodifiers in Production of Concrete for Transport Construction, in Nauchnye trudy OAO TsNIIS (Nauchno-issledovateVskii institut iransporinogo stroilel'stva) (Transactions of the OAO Research Institute of Transport Construction), Tsernant, A.A., Ed. Moscow: Research Institute of Transport Construction, 2008, pp. 41–48.

Tevyashev.A.D. and Shitikov, E.S., On the Possibility of Controlling the Properties of Cement Concretes with the Use of Nanomodifiers. Vost.-Evr. Zh. Peredovykh TekhnoL, 2009, nos. 4/7, 2009, pp. 35-40.

Svatovskaya, L.B., Solov'eva, V.Ya. Komokhov, P.G., Stepanova. I.V. and Svcheva. A.M. Rf Patent 2256629,2004.

Korobov, N.V., Kotorazhuk, Ya.D. and Starchukov, D.S., RF Patent 2331602, 2007.

Roddy, C.W., Chatterji, J. and Cromwell, R. Well Treatment Composition and Methods Utilizing NanoParticles, US Patent 7559369. 2009.

Potapov, V.V., Allakhverdov, G.R., and Serdan, A.A. (J.) et al., Preparation of Aqueous Silica Sols by Membrane Concentration of Hydro-thermal Solutions, Khim. Tekhnol. (Moscow), 2008, no. 6, pp. 14–22.

Generalov, M.B., Kriokhimicheskaya nanolekhnologiya (Cryochemical Nanotechnology), Moscow: Aka-demkniga, 2006.

Brazhnikov, S.M., Generalov, M.B., andTaitnev, N.S., Vacuum Sublimation Technique for Preparing Ultradispersed Powders of Inorganic Salts, Khim. Mashinoslr. (Moscow), 2004, no. 12, pp. 12–15.